Dry deposition processes on urban and suburban surfaces: modelling and validation works

M. Giardina[a,*], A. Donateo[b], P. Buffa[a], D. Contini[b], A. Cervone[c], C. Lombardo[c], F. Rocchi[c]

[a] Department of Engineering, University of Palermo, Viale delle Scienze, Edificio 6, 90128 Palermo, Italy
[b] Institute of Atmospheric Sciences and Climate, ISAC-CNR, str. prov. Lecce-Monteroni, km 1,2, 73100 Lecce, Italy
[c] Italian Agency for New Technologies, Energy and Sustainable Economic Development (ENEA), Via Martiri di Monte Sole, 4, 40129 Bologna, Italy

Abstract

Dry deposition process is one of the important pathways for the removal of particles from atmosphere. It is the result of a combination of different environmental and physical factors as atmospheric conditions, particle properties, characteristics of the canopy. For this latter factor, urban canopy represents unevenly combinations of different types of surface elements that increases the complexity of phenomena that influence deposition processes. Therefore, particle dry deposition on urban surfaces is not easy to configure and, although empirical or semi-empirical models in literature have been developed to address this aspect, there is not standardized and commonly accepted criteria. To overcome this issue, a comparison work has been performed between different models and measurement data by experimental campaigns covering for different surface roughness conditions, i.e. from the patchy Venice surface to the suburban area of Maglie and Lecce, or near urban zone for Bologna. This activity has also included other cities in the world. Giardina et al. (2017b) model, by using two different Brownian diffusion resistance, seems to capture the main dry deposition processes for the examined contexts.

1. Introduction

Urbanization and industrialization are the cause of the formation of pollutants that are deposited on trees, grass, crops, water bodies, and buildings, generating significant environmental impacts. In case of routine emissions, or releases due to nuclear power plant accidents or, more generally, incidents involving the release of hazardous substances a key challenges are the characterization of the specific pollutants that are released as well as studying the dispersion and deposition phenomena. Risk assessment for pollution from hazardous substances is necessary for mitigation strategy formulation and development of policies by decision makers for health protection at regional and national levels.

Dry deposition process, one of the important pathways for the removal of particles from atmosphere, is the result of a combination of different environmental and physical factors as atmospheric conditions, particle properties, characteristics of the canopy. For this latter aspect, the urban canopy represents unevenly combinations of different types of surface elements that increases the complexity of the involved phenomena that influence particle depositions.

Smooth surfaces tend to have lower deposition rates per unit area than rougher surfaces. Such relatively small deposition rates are reported by Roed (1983) for radioactive particles surface deposition as Cs137, on vertical walls, in Denmark. The Author reports the results of nine samples for a brick wall with a range of wet/dry deposition velocities 0.003 to 0.07 cm/s, four samples for a plastered wall with a range of 0.014 to 0.085 cm/s, and only one sample, in an area sheltered from wet deposition, with a dry deposition velocity of 0.003 cm/s.

Nicholson (1987) reported similarly small deposition rates for deposition of Cs134 and Cs137 particles to roof and building materials in England. Although the data set was small, the results were consistent with lower deposition velocities over smoother surfaces.

In (Papastefanou, 2008) an up-to-date summary of knowledge about depositions of radioactive aerosols is provided. Experimental deposition velocities highlighted for Be7 particles variations from 0.1 to 3.4 cm/s, Pb210 from 0.7 to 1.1 cm/s and Cs137 from 1.3 to 6.3 cm/s. These data refer mostly to temperate latitudes of the Northern Hemisphere, e.g. at Oak Ridge, Tennesse (Mahoney, 1984), Norfolk, Virginia (Todd et al., 1989), New Haven, Connecticut (Turekian et al., 1983), Detroit, Michigan (McNeary and Baskaran, 2003), Quillauyte, Washington (Crecelius, 1981), Munich, Germany (Rosner et al., 1996).

Tai et al. (1999) highlighted that particles less than 10 μm contributed to only a small fraction (<10% in mass) of the dry deposition fluxes, both in urban and non-urban locations. These calculations are extremely sensitive to the end-point particle diameter since the dry deposition velocity for a particle of 1 μm in diameter is approximately 100 times smaller than a 10 μm particle, so the concentration of 10 μm particles is 100 times smaller than the concentration of 1 μm particle, if the flux is the same (Holsen and Noll, 1992; Lin et al., 1994; Lee et al., 1996; Ki et al., 2007). Consequently, particles larger than 10 μm in diameter are

* Corresponding author: Mariarosa Giardina, Department of Engineering, University of Palermo, Italy. E-mail address: mariarosa.giardina@unipt.it.

responsible for the majority of dry deposition fluxes, but these particles have a smaller influence on the total airborne concentration (Johnson and Davidson, 2019).

In urban areas, measurements of particle vertical turbulent fluxes are a powerful tool to characterize road traffic pollution or, more in general, urban emissions and the dynamics of particles in the urban surface layer (Contini et al., 2012; Deventer et al., 2015), which allows us to better characterize the exchange of particles between a city and the atmosphere. Diurnal evolution of the particle number concentration and flux for small particles (0.25 μm in diameter), as reported in Conte et al. (2018), shows a clear correlation with anthropic activities (mainly road traffic). The particles fluxes were upward on average, even though small net deposition was observed for larger particles. The city is a continuous source of particles of small size. Others studies of urban deposition rates of hydrocarbons and metals show variations that largely reflect the influence of local sources on ambient airborne contaminant concentrations (Azimi et al., 2005).

Roupsard et al. (2013) studied dry deposition velocities of submicron aerosols on horizontal and vertical urban surfaces of glass, cement facing by using wind tunnel experiments. On horizontal surfaces, dry deposition velocity varies from 0.0014-0.0045 cm/s on conventional glass to 2.8-1.25 cm/s on synthetic grass.

The approach for determining deposition rates has several limitations for urban canopies. Total deposition on the various urban surfaces scales with the available surface areas. Considering the total deposition per unit horizontal area, grass and trees have relatively high deposition rates compared to smooth surfaces. To that extent, modeling the variations in surface deposition require considering interactions of surface roughness and local air circulation.

Therefore modelling of dry deposition phenomena over urban canopies is not easy to configure and, although empirical or semi-empirical models have been developed to address this complex aspect, there is not standardized and common accepted criteria proposed in literature (Droppo, 2006). Indeed, their application remains valid for specific conditions and if the data meet all of the assumptions required by the data used to define the models.

To overcome this issue, a comparison work has been performed between different deposition velocity models and data from several experimental campaigns, covering different surface roughness conditions, i.e. from the patchy Venice surface to the suburban area of Maglie and Lecce, or near urban zone for Bologna. This activity has also included other cities in the world compared to Italy. Giardina et al. (2017b) model, by using two different Brownian diffusion resistance, seems to capture the main dry deposition processes for the examined urban canopies.

2. The main phenomena in dry deposition processes

In atmospheric models, the Surface Layer (SL) is the air layer over the surface whose properties are largely controlled by the local surface fluxes. The strict definition of the surface layer is a fully turbulent layer over homogenous surfaces under steady-state conditions. With this surface layer, a second layer is designated that refers to the laminar, or near-laminar, flow that occurs immediately over the surfaces. This layer, in the literature, is also referred to as the “quasi-laminar sublayer” or “deposition layer”.

The main transport processes, that occurr within the above layers, are:

- transport due to atmospheric turbulence in SL. This process is independent of the physical and chemical nature of the pollutant and it depends only the turbulence level;
- diffusion in the thin layer of air which overlooks the air-ground interface (i.e. quasi-laminar sublayer). The dominant component becomes molecular diffusion for gasses, Brownian motion for particles and gravity for heavier particles;
- transfer to the ground. This component exhibits a pronounced dependence on surface type with which the pollutant interacts (i.e. urban context, grass, forest, etc..).

Therefore, dry deposition phenomena involve three sequential sets of processes:

1. through the turbulent SL, the particle moves by the combined effects of eddy diffusion (i.e., carried by turbulent movements of air) and gravity.
2. in quasi-laminar surface layer, the particle can reach the surface by molecular diffusion, interception, or impaction.
3. near the surface, retention or rebound depends on a combination of surface and impact properties.

It is worth to note that the deposition process changes quite a lot over the year, for example due to the seasonal variation of vegetation (with or without leaf) or over the day in connection with meteorological conditions (e.g. influence of temperature on leaf stoma).

2.1 Transport for atmospheric turbulence in SL

Eddy diffusion refers to the transport resulting from turbulent movements in the air that play a pivotal role in determining the vertical transfer of momentum, heat and mass in the Atmospheric Boundary Layer (ABL), that usually encompasses the lowest tens to hundreds of meters in the atmosphere over the earth's surface (Garratt, 1992). It is widely studied in boundary-layer meteorological modeling, however its impact on dry deposition has not been well understood and characterized.
In approximately the lowest 10% of the ABL (layer SL), the vertical fluxes of transferred quantities are nearly constant with height and can be represented quite successfully by formulations based on the Monin-Obukhov (M-O) similarity theory (Stull, 1988; Högström, 1988, 1996; Foken, 2006).
Under the assumption of steady state between generation, dissipation and transport of the turbulent eddies across the SL, the M-O similarity theory describes relationships between vertical profiles and fluxes for momentum and scalar quantities (i.e., heat and trace constituents), using a metric called Monin-Obukhov length, L (Garratt, 1992):

$$\mathrm{L} = \frac{u_*{}^3 c_p \rho_a \overline{T}}{k\, g\, H} \tag{1}$$

where $\overline{T}$ is the average temperature in SL (K); ρ_a air density (g/cm^3); c_p specific heat at constant pressure [J/kg K]; g gravitational constant (cm/s^2); H sensible heat (W/m^2); k von Karman constant set to 0.4 .
The parameter L is a measure of atmospheric stability. It varies from small negative values in extremely unstable atmospheric conditions to negative infinity, as the atmospheric stability approaches neutral from unstable (neutral conditions L = ∞). In extremely stable conditions, L is small and positive.

2.1.1 Friction velocity and wind speed

The friction velocity is derived from the atmospheric boundary layer similarity theory proposed by Monin and Obukhov (1954). The basic hypothesis of the similarity theory is that a number of parameters in the atmospheric layer near the ground, including the wind profiles, should be universal functions of the friction velocity, the length L, and the height z above ground.
Usually, the ratio z/L is related to atmospheric stability. When z/L is negative and large the atmosphere is extremely unstable, if z/L is near zero, the atmosphere is neutral, if z/L is positive and large the atmosphere is extremely stable.
Under the assumption of continued validity of the M-O flux-gradient relationships in the interfacial sublayer, it is possible to evaluate wind speed profile as follows:

$$\frac{u(z)}{u_*} = \frac{1}{k}\left[\ln\left(\frac{z}{z_0}\right) - \Psi_h(z)\right] \tag{2}$$

with u(z) wind speed at deposition reference height (m/s); u_* friction velocity, (m/s); k von Karman constant; z deposition reference height (m); z_o surface roughness length (m); Ψ_h is a term that takes into account effects of stability on the wind profile.
To calculate the stability function Ψ_h in Eq. (2), Brandt et al. (2002) suggested the following relationship:

$$\Psi_h = -5\frac{z}{L} \qquad \text{with } \frac{z}{L} > 0 \text{ (stable conditions)} \tag{3}$$

$$\Psi_h = e^{\left\{0.598+0.390\ln\left(-\frac{z}{L}\right)-0.09\left[\ln\left(-\frac{z}{L}\right)\right]^2\right\}} \qquad \text{with } \frac{z}{L} < 0 \text{ (unstable conditions)} \tag{4}$$

Under neutral atmospheric stability, Eq. (2) can be simplified as:

$$\frac{u(z)}{u_*} = \frac{1}{k}\ln\left(\frac{z}{z_0}\right) \tag{5}$$

For an aerodynamically rough but relatively flat surface, an extrapolation of the mean wind speed profile downward shows that it reaches zero at some distance above the physical surface. The height at which this occurs is called roughness length, z_o. The roughness length is positively correlated with the physical roughness of the surface, although a strict functional relationship between physical roughness measures and z_o do not exist.

The surface roughness length over land depends on the surface cover and land use and is often difficult to estimate (WMO, 2010). A way of determining z_o is by a visual survey of the terrain around the wind station with the help of the table below, the validity of which has been corroborated (Davenport et al., 2000). Tab. 1 reports Davenport classification of terrain roughness, z_o, for different urban configurations. Other studies have found that the surface roughness length tends to be about one-tenth of the dimensions of the surface elements (Sutton, 1953; Stull, 1988).

In environments such as over agricultural crops and forest and urban canopies, the practice is to displace the entire velocity profile upward such that the height at which velocity profiles reach zero is the sum of a canopy roughness length, z_o, and displacement height, d, defined as zero plane displacement. Fig. 1 reports a generalized mean wind velocity profile in a developed urban area and the zero-plane displacement length, d, for this configuration.

Consequently, Eq. (5) is modified as follows:

$$\frac{u(z)}{u_*} = \frac{1}{k}\ln\left(\frac{z-d}{z_0}\right) \tag{6}$$

2.2 Transport to Brownian motions

Brownian motion is usually assumed to dominate the diffusion processes in the quasi-laminar surface layer. However, there is the possibility that phoretic forces can locally influence dry deposition fluxes.

Particles in the range of 0.001 to 0.1 (µm) (ultrafine particles) move like gaseous molecules in flowing air (i.e., they exhibit rapid random Brownian motion). The motion causes them to collide with any nearby surfaces. Ultrafine particles tend to adhere to these surfaces as the result of intermolecular forces. This mechanism tends to be an effective deposition process with very small particles depositing at rapid rates on the nearest available surfaces. Under some circumstances, this diffusion mechanism can continue to be the dominant deposition process for particles >0.1 µm.

2.3 Gravitational settling

Gravitational settling is the downward motion of particles that results from the gravitational attraction and it is the dominant process for the dry deposition of the larger particles of about 10 µm.

Particulate sizes, densities, and shapes largely define gravitational settling rates.

The settling velocity for particles, v_s, can be computed using a modified form of Stokes Law (Hanna et al., 1982):

$$v_s = \frac{C_c\, d_p{}^2 g(\rho_p - \rho_a)}{18\mu_a} \tag{7}$$

where ρ_p is the particle density, (g/cm^3); μ_a is the air dynamic viscosity (g/cm s); d_p is the particle diameter, (cm); and C_c is the Cunningham factor.

The Cunningham factor can be expressed as (Seinfeld and Pandis, 1998):

$$C_c=1+\frac{\lambda_a}{d_p}\left(2.514+0.8\, e^{\frac{-0.55 d_p}{\lambda_a}}\right) \tag{8}$$

where λ_a is the mean free path of air (cm).

Non-spherical particles fall at slower rates. For materials with equivalent densities, the change in settling velocities is less than 30% for ellipsoid and cylinder shapes. To account for shape effects, an aerodynamically equivalent diameter (Jennings and Parslow, 1988; Reid et al., 1994) is frequently used to define the settling velocity of a particle.

3. Urban deposition models

An urban area represents a complex context for assessment of potential exposures from an atmospheric release and, in this filed, dry deposition models are too simple for application to the urban environment

(Cherin et al., 2015). Their classical approaches (Wesely and Hicks, 2000; Petroff et al., 2008), which are inherited from semi-empirical models, were developed for deposition over vegetated surfaces, bare soil or water, and therefore they fail to represent the complexity of the dry deposition processes over an urban canopy.

A review of dry (and wet) deposition computational methods was conducted for radioactively contaminated particles (in the range 0.1 to 10 μm) by the Atmospheric Dispersion Modeling Liaison Committee (NRPB, 2001). They are recommend values and methods to estimate deposition rates and special parameter limits to extrapolate the dry deposition model to an urban environment. However, neither of these reviews addressed the issues of the applicability of the dry deposition models to non-ideal conditions such as the aerodynamically very rough surfaces encountered in an urban environment.

Resistance-based approaches are widely used as a basis for dry deposition formulations. This approach, explained in more detail below, has the advantage of providing a means of combining a number of the processes controlling dry deposition into a single formulation.

In one of the early implementations, Sehmel and Hodgson (1978) proposed an empirical model based on curve fits to wind tunnel deposition results for a range of soil surface covers. Their model combined empirical data with the theory for molecular diffusion of very small particles and gravitational settling rates for larger particles. The Authors also demonstrated the importance of considering the density of the particles in the dry deposition computation. Subsequent applications have included air quality (e.g., chemicals and trace metals), health physics (radionuclides), and acid rain models.

Detailed models, that address the processes leading to exposures in an urban environment, have been developed for radiological exposures (Jones et al., 2006).

Eged et al. (2006) used a Monte Carlo approach to evaluate potential radiological doses in urban environments. The results show that urban dose computation models provide some results that are the same and some that are not.

Based on their experimental results, Chen et al. (2012) developed a relationship between TSP (Total Suspended Particulate Matter) deposition velocity and meteorological parameters. The experimental campaigns were conducted in locations near Guangzhou, China, during dry season. The dry deposition velocity equation is a function of the wind speed, the relative humidity, and air temperature.

Noll et al. (2001) correlate the particle deposition velocity with Stokes settling velocity, friction velocity, dimensionless inertial deposition velocity, and dimensionless Brownian diffusion deposition velocity by using 20 atmospheric samples collected at flow Reynolds numbers ranging from 9000 to 30,000 and related to particle size of range 1÷100 μm. Some samples were collected on the roof of a four-story building (12 m height) located in a mixed institutional, commercial, and residential area on the south of Chicago. A model was developed using a least square procedure to fit a sigmoid curve to ambient data, similarly to one developed for deposition in a vertical pipe (Muyshondt et al., 1996).

A parameterization of particle dry deposition has been developed in (Zhang et al., 2001) for different surfaces and meteorological variables. It includes deposition processes, such as, turbulent transfer, Brownian diffusion, impaction, interception, gravitational settling, particle rebound and also particle growth under humid conditions. The parameters in dry deposition velocity calculations are different on the basis of 12 land use categories, including urban area, and five seasonal categories.

3.1 Resistance approach to describe dry deposition processes

In mechanistic or process-based dry deposition models, an electrical resistance-based approach is widely used to parameterize the dry deposition velocity (Venkatram and Pleim, 1999; Zhang et al., 2001; Giardina et al. 2017a; Giardina and Buffa, 2018).

By considering that the reciprocal of the dry deposition velocity, v_d, is the overall resistance to the mass transfer, the influence of the various phenomena on the deposition velocity can be expressed in terms of an electrical analogy.

Giardina et al. (2017b) proposed a new approach to evaluate the total resistance r_t for urban rough surfaces.

In SL the aerodynamic resistance, r_a, is connected in series with the resistance across the quasi-laminar sublayer, r_{ql}, to take into account mechanisms of diffusion by Brownian motion and turbulent phenomena (Fig. 2). Accordingly, the overall resistance, r_t, is evaluated by the using the following equations:

$$r_t = \mathrm{r_a} + \mathrm{r_{ql}} \tag{9}$$

Relationships for aerodynamic resistances r_a are based on surface layer parameterizations from M-O similarity theory:

$$r_a = \frac{\ln\left(\frac{z}{z_0}\right) - \psi_h}{k u_*} \tag{10}$$

In Eq. (10), Eq.s (3) and (4) can be used to calculate the stability function Ψ_h.
The resistance r_{ql} is evaluated by considering two resistances in parallel, that is: resistance r_{bd}, which represents the Brownian diffusion process; and resistance r_i, which allows to treat turbulent and impaction phenomena. The resistance r_i is evaluated by considering two resistances in series: r_{ii} to take into account inertial impact conditions; r_{ti} to consider effects resulting from turbulent impaction. This last assumption allows to take into consideration the reciprocal influence of the two impact processes on dry deposition efficiency.
The Authors assumed the expression reported in Eq. (11) for the resistance r_{bd} as suggested in (Wesely and Hicks, 2000; Paw, 1983; Hicks et al., 1987; Pryor et al., 2009; Kumar and Kumari, 2012; Giardina and Buffa, 2018):

$$r_{bd} = \frac{1}{u_* Sc^{-2/3}} \tag{11}$$

where Sc is the Schmidt number evaluated as follows:

$$Sc = \frac{\nu_a}{D} \tag{12}$$

with ν_a the air kinematic viscosity (m^2/s) and D the Brownian diffusivity of air (m^2/s).
To evaluate the resistance for inertial impact process r_{ii}, it is used the following relationship valid for rough surfaces:

$$r_{ii} = \frac{1}{u_* \left(\frac{St^2}{St^2+1}\right) R} \tag{13}$$

where St is the Stokes number:

$$St = \frac{{u_*}^2 v_s}{\upsilon_a} \tag{14}$$

The parameter R in Eq. (13) is the particle rebound evaluated as follow:

$$R = e^{(-b\sqrt{St})} \tag{15}$$

where b is assumed equal to 2, as suggested in (Nemitz et al., 2002)
Empirical relations of turbulent deposition are typically presented in terms of the dimensionless particle relaxation time τ_+:

$$\tau_+ = \tau \frac{u_*^2}{\nu_a} \tag{16}$$

where τ is the particle relaxation time defined, for a spherical particle, as follows:

$$\tau = \frac{d_p^2 \rho_p C_c}{18 \mu_a} \tag{17}$$

Various models predict a functional dependence of resistance turbulent impact phenomena, r_{ti}, on τ_+ as follows:

$$r_{ti} = \frac{1}{u_* m \tau_+^n R} \tag{18}$$

Various works have been performed to evaluate m and n parameters, and these constants have been revised by fitting some data reported in literature for roughness surfaces (Giardina et al., 2018). The results were m=0.1 and n=0.5.

Venkatram and Pleim (1999) proposed the following expression for dry deposition velocity of particles that is consistent with the mass conservation equation:

$$v_d = \frac{v_s}{(1 - e^{-r_t v_s})} \tag{19}$$

In the light of the above considerations about the total resistance r_t, Eq. (19) can be rewritten as follows:

$$v_d = \frac{v_s}{1 - e^{-\left\{v_s\left[r_a + 1/\left(\frac{1}{r_{db}} + \frac{1}{r_{ii} + r_{ti}}\right)\right]\right\}}} \tag{20}$$

where r_{db}, r_{ii}, and r_{ti} are evaluated by Eq.s (10), (11), (13), and Eq. (18) with m=0.1 and n=0.5.

3.2 Considerations about Brownian diffusion resistance

In literature, various models have been developed to predict functional dependence of Brownian diffusion resistance, r_{bd}, from Sc number and friction velocity, u_*, however they cannot be extended for urban conditions.

Some Authors defined a Brownian diffusion resistance dependency on roughness Reynolds number defined as $Re_* = u_* z_o/\nu$. For example, in (Chamberlain et al., 1984) experiments were carried out to study diffusive transfer to bluff roughness elements that can be compared to urban and suburban conditions.

Radioactive gases and labelled particles were used in wind tunnels to measure the effects of Re_* and Scnumbers on transport to surfaces with widely spaced roughness elements. It is highlighted that deposition of larger particles is dominated by the effects of bounce off, which depends on surface conditions.

In this field, research activities have been carried out to define a new formulation that is capable to perform predictions for different typologies of urban area and small particle diameters (Giardina et al., 2018).

Fitting approach was performed on parameters that associate Brownian diffusion resistance to Re_* and Sc. This analysis was carried out by using experimental data of dry deposition velocity for different rough surfaces (Chamberlain et al., 1984, Pryor et al., 2009; Donateo and Contini, 2014).

The following relationship was obtained:

$$r_{bd} = \frac{1}{u_* Sc^{-0.5} Re_*^{-0.05}} \tag{21}$$

4. Validation works of dry deposition velocity modeling for Italian cities

The validation works have been performed by using experimental campaigns carried out by researchers from Institute of Atmospheric Sciences and Climate (ISAC), Italian National Research Council (CNR), unit of Lecce, covering for different surface roughness conditions of urban-suburban Italian areas (Donateo and Contini, 2014).

For the experiments, performed between 2004s and 2009s, the displacement height, d, and the roughness length, z_0, are reported in Tab. 2. These data have been evaluated from micrometeorological measurements, following a method reported in (Toda and Sugita, 2003) which uses similarity relationship for sonic temperature and vertical wind component.

Measured dry deposition velocities have been compared with predictions of models reported in (Giardina et al., 2017b), (Chen et al., 2012), (Noll et al., 2001), and (Zhang et al., 2001), by adopting the roughness lengths reported in Tab. 2. For Chen et al. (2012) model, average values of wind velocity, temperature and relative humidity measured during the experimental campaigns were used, where available. The model of Zhang et al. (2001) was applied by using the parameters imposed for urban land use categories, as for roughness length, z_o, imposed by the authors to 1 m.

In all figure captions, NNR index (Attilio et al., 1993), which allows comparisons of model performances independently of the shape of the set of measured data, was evaluated as follows:

$$\mathrm{NNR} = \frac{\sum_i \left(1-\hat{k}_i\right)^2}{\sum_i \hat{k}_i} \tag{22}$$

where

$$\hat{k}_i = e^{-|ln k_i|} \tag{23}$$

$$k_i = \frac{v_{dp_i}}{v_{do_i}} \tag{24}$$

being v_{dp_i} and v_{do_i} predicted and observed deposition velocities, respectively.
NNR index is the normalized mean square error of the distribution of the normalized ratios $\hat{k}_i$ compared with the ideal distribution $\hat{k}_i = 1$.

4.1 Maglie suburban site (South-Eastern Italy)

The measurement site, located in NE boundary of the town of Maglie (LE) in the Apulia region of Italy (40°07’38.39’’N, 18°17’59.50’’E), can be considered a suburban site influenced by an industrial area. The town is extending mainly in the sector of wind direction between SE and SW and the country side is in the sector between NNO and E. The site is characterized by presence of small buildings (1-2 floors) and roads with relatively high traffic volume (Donateo et al., 2006).
$PM_{2.5}$ monitoring campaigns were performed mainly from November to January in 2004, 2006 and 2007. Fig.s 3 and 4 show the deposition velocity as function of friction speeds u_* and unstable and stable conditions, respectively. Comparisons between experimental data reported in (Donateo and Contini, 2014), carried out by ISAC-CNR unit of Lecce, and predictions obtained by applying models reported in (Giardina et al., 2017b), (Chen et al., 2012), (Noll et al., 2001), and (Zhang et al., 2001), for particle diameter d_p of 2.5 μm, are shown.
Giardina et al. (2017b) model has been tested by using Eq. (20) and relationships reported in Eq.s (11) and (21) for the Brownian diffusion resistances.
Analyzing results, Noll et al. (2001) and Zhang et al. (2001) models overestimate experiments with wind friction velocities higher than 0.2 m/s, whereas Chen et al. (2012) model overestimates experiments for all wind friction velocities. Giardina et al. (2017b) model shows a good agreement with the experimental data if it is applied with the Brownian diffusion resistances reported in Eq.s (11) and (21), and the two predictions result very close both for unstable and stable conditions. This result is confirmed by NNR index values.

4.2 Venice urban site (North-Eastern Italy)

Measurements were performed at a background site placed on Venice lagoon (Donateo et al., 2012). The measurement site (45°29’09.5’’N, 12°24’12.7’’E) was a field located at about 8 km NE of the Venice town. This site was located very close (about 5 m) to the water lagoon at the W-SW side, while, in the other directions (selected for this work), it was characterized by land for about 1-2 km with short vegetation, some small trees, and one or two-floor houses, although channels and water were also present in this area.
Monitoring campaigns of $PM_{2.5}$ concentrations and flux measurements were performed during the summer 2004, winter 2005 and spring 2006.
Fig.s 5 and 6, that report the deposition velocity as function of friction speed, refer to instability and stability atmospheric conditions, respectively.
These figures shown comparisons among experimental data carried out by ISAC-CNR and elaborated in this work, and predictions obtained by using models reported in (Giardina et al., 2017b), (Chen et al., 2012), (Noll et al., 2001), and (Zhang et al., 2001), for particle diameter d_p of 2.5 μm.
(Giardina et al., 2017b) model has been tested by using Eq.s (11) and (21).
Very high differences can be highlighted between dry deposition velocities experimental data and the predictions of Zhang et al. (2001) and Noll et al. (2001) models, both for unstable and stable conditions and wind friction velocities higher than 0.2 m/s. Chen et al. (2012) model overestimates the observations data for all wind friction velocities.
The predictions obtained by Giardina et al. (2017b) model, applied with Eq.s (11) and (21), show a good agreement with experimental data.

4.3 Bologna industrial district (Central Italy)

The measurement site was near the incinerator plant for the city of Bologna, (44°31'17.59''N, 11°25'53.48''E). The data refer to experimental campaigns performed in summer 2008 and winter 2009. Fig.s 7 and 8 report the deposition velocity experimental data as function of friction velocity for instability and stability atmospheric conditions, respectively.
Comparisons between experiments reported in (Donateo and Contini, 2014), and results obtained by using models reported in (Giardina et al., 2017b), (Chen et al., 2012), (Noll et al., 2001), and (Zhang et al., 2001) are shown.
The experiments reported in (Donateo and Contini, 2014) were carried out from June to July 2008, and January to March 2009 for particle diameter d_p of 0.045 μm.
High differences can be highlighted between dry deposition velocities experimental data and the predictions of Noll et al. (2001) and Chen et al. (2012) models.
As NNR index values pointed out, the predictions of Zhang et al. (2001) and Giardina et al. (2017b) models, this last applied with Eq. (21), show very good agreement for all experiments and unstable conditions (Fig.7). For stable conditions (Fig. 8) the best predictions are attributed to (Giardina et al., 2017b) model applied both with Eq.s (11) and (21).

4.4 Lecce suburban site

Experimental campaigns were performed during spring/summer of 2005. $PM_{2.5}$ concentrations and fluxes were measured.
The site was the experimental field of the Lecce Unit of ISAC-CNR placed inside the University Campus (40°20'10.8''N, 18°07'21.0''E) and located at about 3.5 km SW from the town of Lecce. It is a rectangular field with a major side of about 200 m characterized by short vegetation, with two contiguous sides surrounded by small trees.
The urban background area is characterized for at least 1 km in all directions by the presence of patches of trees (8–10 m tall) and small two-story buildings and some roads with no industrial releases nearby.
Due to the proximity of urban areas, the site can be categorized as an urban background area. Measurements were taken at 10 m above the ground.
Fig.s (9) and (10) show the deposition velocity as function of friction speeds for unstable and stable conditions reported in (Donateo and Contini, 2014), and predictions obtained by applying the models reported in (Giardina et al., 2017b), (Noll et al., 2001), and (Zhang et al., 2001).
Analyzing results, Noll et al. (2001) model allows very high underestimations rates of experimental data with friction velocities higher than about 0.2 (m/s), both unstable and stable conditions.
Giardina et al. (2017b) model, applied with Eq.s (11), and (21) show a good agreement with all experimental data. The curves result very close each other, both for unstable and stable conditions.

5. Validation work of dry deposition velocity on United States urban areas

Dry deposition phenomena modelling on urban canopies is limited and, although empirical or semi-empirical models have been developed to address this complex issue, there is no universal acceptance criteria. Therefore, it can be said that the models proposed in literature are not capable of representing particle dry deposition for several categories of pollutants and different urban surface conditions.
In order to overcome this issue, validation works have been extended to experimental campaigns on different urban canopies compared to Italy.
In this section the results obtained on typical United States urban areas are shown and discussed.
It is to be noted that the roughness length z_0 for the examined urban areas were evaluated by using Devenport classification reported in Tab. 1 if not reported by the Authors. (Zhang et al., 2001) model was applied by using the parameters imposed for urban land use categories and z_o =1 m as suggested by the Authors.

5.1 Experimental data of Noll et al. (2001)

Four sampling campaigns conducted at Chicago are described in (Noll et al., 2001). The data were collected on the roof of a four-story building (12 m height) located in a mixed institutional, commercial, and residential area on the south of Chicago.

The building is located on the IIT (Illinois Institute of Technology) campus, which is located 5.6 km south of Chicago's center and 1.6 km west of Lake Michigan. The IIT campus consists of predominately low rise buildings, landscaped areas, and asphalt parking lots. The atmospheric particle mass size distribution and dry deposition flux were measured simultaneously with a wide range aerosol classifier (WRAC) and a smooth greased surface.

The 20 sets of atmospheric measurements that were used to develop Noll et al. (2001) model were grouped into 4 Reynolds number classes of 9,000–13,000 (class I), 13,000–17,000 (class II), 17,000–21,000 (class III), and >21,000 (class IV). The average wind velocities for the 4 classes were 3.42, 4.64, 5.82, and 7.87 m/s.

Fig. (11) reports the experimental dry deposition velocity as function of particle diameters in log-log graph. Comparisons with predictions obtained by using models reported in (Giardina et al., 2017b), (Noll et al., 2001) and (Zhang et al., 2001) are also shown.

The models reported in (Giardina et al., 2017b) and (Noll et al., 2001) were applied by using the class "Very rough" for the terrain roughness reported in Tab. 1 (z_0=0.5). Moreover Noll et al. (2001) model is used with Reynolds number of 15000. The friction velocity was imposed equal to 20 cm/s.

As expected, Noll et al. (2001) predictions show a good agreement with the experimental data reported in Fig. (11), while the model of Giardina et al. (2017b), applied with Eq.s (11) and (21), underestimate the experimental data if the particle diameter is greater than 10 μm.

(Zhang et al., 2001) predictions give a good agreement with the experimental data. However, it shows the highest deposition velocity values among models' applications for particle diameters d_p less than about 10 μm.

5.2 Experimental data of McNeary and Baskaran (2003)

The depositional fluxes in the bulk and dry fallout as well as the concentrations of Be7 and Pb210 in aerosols were measured for a period of 17 months at Detroit, Michigan. The concentrations contributed 2.1–19.8% and 3.6– 48.6% of the bulk depositional fluxes.

The bulk depositional fluxes varied between 3.11 and 63.0 dpm/cm^{2}yr and 0.35 and 10.3 dpm/cm^{2}yr, respectively, and this variability is attributed to the frequency and amount of precipitation and seasonal variations in the depositional fluxes.

The sampling site is one of the air monitoring network stations operated by the Wayne County Air Quality Management Division and jointly operated by the Wayne County and the Michigan Department of Environmental Quality (MDEQ), under cooperative agreement with the U.S. Environmental Protection Agency (EPA).

A bulk rain collector (200-L polyethylene drum with surface area of 2800 cm^2) was deployed in September 1999 at a site in the southwest area of Detroit, Michigan (42° 250' N; 83° 10' W; 175 m above mean sea level) at about 1 m above the ground to prevent the resuspension of dust particles getting into the collector. The lid of the bulk collector was deployed as the dry collector in October 1999 on the roof of a building at the same site at about 4 m above ground.

The bulk rain samples were collected after each major precipitation event or once in about a month and after about 10 days of dry weather for the dry collector.

The models reported in (Giardina et al., 2017b) and (Noll et al., 2001) were applied by using the class "Skimming" for the terrain roughness reported in Tab. 1.

Fig.s (12), (13) and (14) report comparisons between dry deposition experimental data, during the period from October 1999 to January 2001, and predictions of models proposed in (Giardina et al., 2017b), by using Brownian diffusion resistance Eq.s (11) and (21), and (Zhang et al., 2001), for particle diameters d_p = 0.1 and 1 μm, respectively.

The wind speeds used for model applications are related to measurements performed by meteorological station located near Detroit airport (Windsor) for the examined periods. This station is the closer site to the dry deposition flux measurement point.

As we can see in all figures, as expected the calculated dry deposition rate increases with increasing of the particle diameter.

For some periods, (Giardina et al., 2017b) model with Eq. (11) and particle diameter of 0.1 μm (Fig. 12) underestimates the dry deposition velocity, whereas the predictions are improved if the model is used with Eq. (21) (Fig. 13).

The predictions, obtained by using (Zhang et al., 2001) model and reported in Fig. 14, overestimate the experimental data for particle diameter of 1 μm and allow a good agreement for particle diameter of 0.1 μm.

It should be highlighted that the experimental measurements were carried out also during rainy days, so these weather conditions can only increase deposition processes compared to dry deposition phenomena. Therefore, the above described results shall be assessed also in relation to this last consideration.

6. Validation work of dry deposition velocity on France suburban-urban areas

Experimental campaigns reported in (Connan et al., 2018) were conducted from December 2010 to August 2011 in the car park of Cherbourg, France (49.6348 ° N-1.6456 ° W), on a site characteristic of an urban zone. The sonic anemometer was placed 1 m from the ground. The friction wind u_* was calculated from the measurements at the time of the experiment that was taken systematically (i.e. over a period of about 10 to 30 min).

Measurements made for different relative contact surfaces. The classical sample with a normal density was defined as a grass with a relative contact surface (RCS) of 1; samples with 2 times smaller RCS (RCS = 1/2) and 3 times smaller RCS (RCS = 1/3) were also prepared by removing 1 strand of grass out of 2 or 1 strand of grass out of 3 for a given area (20 x 20 cm).

The experimental results are reported in terms V_d/ u_* parameter as function of particle diameters as shown in Fig. 15.

Experimental results show that v_d/ u_* varies in a range of 2 to 6 10^{-3} for particle diameters from 0.2 to 1.2 μm. Beyond 1.2 μm the v_d/ u_* ratio increases rapidly with a value of 5.4 10^{-2} to 7.8 μm.

Fig. (15) also shows the predictions obtained by applying the models reported in (Giardina et al., 2017b) and (Zhang et al., 2001). Giardina et al. (2017b) model has been tested by using Eq. (20) and relationships reported in Eq.s (11) and (21) for the Brownian diffusion resistances.

Good predictions are obtained by using (Giardina et al., 2017b) model, with Eq. (21), and (Zhang et al., 2001) model, even if this last shows the best performance.

7. Conclusion

Dry deposition process is the result of a combination of different factors as atmospheric conditions, particle properties, characteristics of deposition methods as natural surfaces, urban area and water surfaces. Among the many possible configurations, urban canopy represents an uneven combinations of different types of surface elements that increases the complexity of the involved phenomena.

Quantifying the amount of dry deposition is critical since these deposition processes determine the pollutant species' lifetime in air and their input to various ecosystems.

The approach to determine deposition rates has several limitations for urban area. Total deposition on the various urban surfaces scales with the deposition rates and available surface areas. Considering the total deposition per unit horizontal area, grass and trees have relatively high deposition rates compared to smooth surfaces.

Therefore, modeling the variations in surface deposition requires to considere interactions of surface roughness and local air circulation. Dry deposition models are too simple for application to the urban environment (Cherin et al., 2015). Their classical approaches (Wesely and Hicks, 2000; Petroff et al., 2008), which are inherited from semi-empirical models, were developed for deposition over vegetated surfaces, bare soil or water, and therefore they fail to represent the complexity of the dry deposition processes over an urban canopy.

It follows that the modelling of dry deposition phenomena within urban canopies is not easy to configure and, although empirical or semi-empirical models have been developed to address this complex aspect, there is not a standardized and common accepted criteria proposed in literature (Droppo, 2006). Indeed, their application remains valid for specific conditions and if the data in that application meet all of the assumptions required by the models.

To overcome this problem, a validation work of different models has been performed. For this activity, we used the data obtained in experimental campaigns carried out by researchers from ISAC-CNR unit of Lecce, covering for different surface roughness conditions, but also in other parts of the world compared to Italy.

In particular (Giardina et al., 2017b), (Chen et al., 2012), (Noll et al., 2001), and (Zhang et al., 2001) models were tested.

Giardina et al. (2017b) model, by using Eq.s (11), (21) for the Brownian diffusion resistances, seems to capture the main dry deposition processes for the examined urban canopies. However the use of Eq. (21) shows the best agreements for Italian cities, if NNR index is investigated. Moreover, this latter approach can

improve deposition velocity predictions for particles with diameter smaller than 1 μm, as shown by comparisons with the experimental data of (Connan et al., 2018) as reported in Fig. 15.
A good agreement is also obtained by using Zhang et al. (2001) model, especially for particles diameter greater than 2.5 μm and friction velocity of about 0.2 m/s, as shown by dry deposition velocity predictions of experiments reported in (Noll et al., 2001) (Fig. 11). However, overestimations are obtained if it is used for Italian urban areas and friction speeds higher than 0.2 m/s, save for suburban areas such as Bologna and particle diameter of 0.045 μm (Fig.s 7 and 8).

References

Attilio A.P., Mario C.C. 1993. On the use of the normalized mean square error in evaluating dispersion model performance, Atmospheric Environment. Part A. General Topics, Volume 27, Issue 15, 2427-2434

Azimi S., Rocher V., Muller M., Moilleron R., Thevenot D.R. 2005. Sources, distribution and variability of hydrocarbons and metals in atmospheric deposition in an urban area (Paris, France). Sci. Total Environ. 337 (1-3):223-239.

Brandt J., Christensen J.H., Frohn L.M. 2002. Modelling transport and deposition of cesium and iodine from the Chernobyl accident using the DREAM model Atmos. Chem. Phys., 2, 397–417.

Chamberlain A.C., Garland J.A., Wells A.C. 1984. Transport of gases and particles to surfaces with widely spaced roughness elements, AERE Harwell, UK.

Chen L., Shaolin P., Jingang L.,Qianqian H. 2012. Dry deposition velocity of total suspended particles and meteorological influence in four locations in Guangzhou, China. Elsevier Environment science 24 (4), 632-639.

Cherin N., Roustan Y., Musson-Genon L., Seigneur C. 2015. Modelling atmospheric dry deposition in urban areas using an urban canopy approach, Geosci. Model Dev., 8, 893-910.

Connan O., Pellerin G., Maro D., Damay P., Hébert D., Roupsard P., Rozet M., Laguionie P. 2018. Dry deposition velocities of particles on grass: Field experimental data and comparison with models, Journal of Aerosol Science, December 2018, 58-67.

Conte M., Donateo A., Contini D. 2018. Characterisation of particle size distributions and corresponding size-segregated turbulent fluxes simultaneously with CO2 exchange in an urban area. Science of the Total Environment 622–623 (2018) 1067–1078

Contini, D., Donateo, A., Elefante, C., Grasso, F.M. 2012. Analysis of particles and carbon dioxide concentrations and fluxes in an urban area: correlation with traffic rate and local micrometeorology. Atmos. Environ. 46, 25–35.

Crecelius E.A. 1981. Prediction of marine atmospheric deposition rates using total 7Be deposition velocities. Atmos. Environ. 15, 579–582.

Davenport A.G., Grimmond C.S.B., Oke T.R., Wieringa J. 2000. Estimating the roughness of cities and sheltered country. Proceedings 12th Conference on Applied Climatology, Asheville, NC, American Meteorological Society, Boston, 96-99.

Deventer, M.J., El-Madany, T., Griessbaum, F., 2015. One-year measurement of size resolved particle fluxes in an urban area. Tellus 67, 25531–25546

Donateo A., Contini D., Belosi F., Gambaro A., Santachiara G., Cesari D., Prodi F. 2012. Characterisation of PM2.5 concentrations and turbulent fluxes on an island of the Venice lagoon using high temporal resolution measurements. Meteorologische Zeitschrift, Vol. 21, No. 4, 385-398.

Donateo A., Contini, D., 2014. Correlation of dry deposition velocity and friction velocity over different surfaces for PM2.5 and particle number concentrations. Advances in Meteorology, Volume 2014, Article ID 760393, 12 pages.

Donateo, A., Contini, D., Belosi, F. 2006. Real time measurements of PM2.5 concentrations and vertical turbulent fluxes using an optical detector. Atmospheric Environment 40, 1346-1360.

Droppo J.G. 2006. Improved Formulations for Air-Surface Exchanges Related to National Security Needs: Dry Deposition Models U.S. Department of Homeland Security, DE-AC05-76RL01830report PNNL-15876

Eged K., Kis Z., Voigt G. 2006. Review of dynamical models for external dose calculations based on Monte Carlo simulations in urbanized areas. Journal of Environmental Radioactivity 85(2-3):330-343.

Foken T., 2006. 50 years of the Monin-Obukhov similarity theory. Bound.-Layer Meteorol. 119, 431-447.

Garratt J.R., 1992. The Atmospheric Boundary Layer. Cambridge Univ. Press, Cambridge, UK.

Giardina M., Buffa P. 2018. A new approach for modeling dry deposition velocity of particles, Atmospheric Environment, 180 (2018), 11–22.

Giardina M., Buffa P., Cervone A., De Rosa F., Lombardo C., Casamirra M. 2017a. Dry deposition models for radionuclides dispersed in air: a new approach for deposition velocity evaluation schema. Journal of Physics: Conference Series, Volume 923, conference 1

Giardina M., Buffa P., Cervone A., Lombardo C. 2017b. Analisi dei modelli validi per lo studio dei processi di deposizione secca e sui dati meteo previsionali dell'ECMWF, rapporto di ricerca ENEA n. ADPFISS-LPI-092 Rev.0.

Hanna SR., Briggs GA., Hosker RP. 1982. Handbook on Atmospheric Diffusion., DOE/TIC-11223, U.S. Department of Energy, Washington, D.C.

Hicks B.B., Baldocchi D., Meyers T., Hosker R., Matt D. 1987. A preliminary multiple resistance routine for deriving dry deposition velocities from measured quantities, Water Air Soil Poll., 36, 311–330, 1987.

Hicks B.B., Wesely M.L., Durman J.A., Brown M.A. 1982. Some direct measurements of atmospheric sulphur fluxes over a pine plantation. Atmos. Envir. 16:2899-2903.

Högström U., 1988. Non-dimensional wind and temperature pro € files in the atmospheric surface layers: a re-evaluation. Bound.-Layer Meteorol. 42, 55e78.

Högström U., 1996. Review of some basic characteristics of the atmospheric surface € layer. Bound.-Layer Meteorol. 78, 215e246.

Holsen T. M., Noll, K. E. 1992. Dry deposition of atmospheric particles: application of current models to ambient data. Environ. Sci. Technol. 26, 1807-1815.

Jennings B.R., Parslow K. 1988. Particle Size Measurement: The Equivalent Spherical Diameter. Proceedings of the Royal Society of London. Series A 419, 137-149.

Johnson A.J., Davidson C.I. 2019. Measuring atmospheric dry deposition with large surrogate surfaces for improved time resolution, Atmospheric Environment, 198, 489-495.

Jones J.A., Singer L.N., Brown J. 2006. The EXPURT model for calculating external gamma doses from deposited material in inhabited areas. Journal of Environmental Radioactivity 85(2-3), 314-329.

Ki H.S., Kim J.G., Kim K.S. 2007. Study on atmospheric behavior of polycyclic aromatic hydrocarbons in urban area, Environ. Eng. Res. Vol. 12, No. 3, 118-127.

Kumar, R., Kumari, K. M. 2012. Experimental and Parameterization Method for Evaluation of Dry Deposition of S Compounds to Natural Surfaces, Atmospheric and Climate Sciences, 2, 492-500.

Lee W.J., Su C.C., Sheu H.L., Fan Y.C., Chao H.R., Fang G.C. 1996. Monitoring and modeling of PCB dry deposition in urban area. Journal of Hazardous Materials 49(1), 57-88.

Lin J. J., Noll K. E., Holsen T. M. 1994. Dry deposition velocities as a function of particle size in the ambient atmosphere. Aerosol Sci. Technol. 20, 239-252.

Mahoney L.A. 1984. Beryllium-7 deposition to terrestrial vegetation in Tennessee. Ph.D. thesis, Western Kentucky University, Bowling Green, KY.

McNeary D., Baskaran M. 2003. Depositional characteristics of 7Be and 210Pb in southeastern Michigan Journal of Geophysical Research, Vol. 108, NO. D7, 4210, doi:10.1029/2002JD003021, 2003.

Muyshondt A., Arnand N.K., McFarland R. M. 1996. Turbulent Deposition of Aerosols Particles in Large Transport Tubes, J. Aerosol Sci. 24:107– 116.

Nemitz E., Gallagher M. W., Duyzer J.H., Fowler D. 2002. Micrometeorological measurements of particle deposition velocities to moorland vegetation Q. J. R. Meteorol. Soc., 128, 2281-2300.

Nicholson K.W., Davies T.D. 1987. Field measurements of the dry deposition of particulate sulphate, Atmospheric Environment, 21, 1561-1571

Noll KE., Jackson M.M., Oskouie K.A. 2001. Development of an atmospheric particle dry deposition model, Aerosol Science and Tecnology, 35(2), 627-636.

NRPB, National Radiological Protection Board. 2001. Atmospheric Dispersion Modeling Liaison Committee Annual Report 1998/99. NRBT-R322, National Radiological Protection Board, Oxford.

Papastefanou C. 2008. Radioactive Aerosols, Radioactivity in the environment, Elsevier Science Volume 12, 1-171.

Paw U.K.T. 1983. The rebound of particles from natural surfaces. Journal of Colloid Interface Science 93, 442-452.

Petroff, A., Mailliat, A., Amielh, M., and Anselmet, F. 2008. Aerosol dry deposition on vegetative canopies, Part I: Review of present knowledge, Atmos. Environ., 42, 3625–3653.

Pryor S.C. , Barthelmie R. J., Spaulding A. M, Larsen S. E., Petroff A. 2009. Size-resolved fluxes of sub-100-nm particles over forests. Journal of Geophysical Research,114, D18212.

Reid J. S., Cahill T.A., Wakabayashi P.H., Dunlap M.R. 1994, Geometric/aerodynamic equivalent diameter ratios of ash aggregate aerosols collected in burning Kuwaiti well fields, Atmospheric Environment, 28 (13), 2227-2234. doi.org/10.1016/1352-2310(94)90362-X

Roed J. 1983. Deposition Velocity of Caesium-137 on Vertical Building Surfaces. Atmospheric Environment, 17(3), 663-664

Rosner G., Hotzl H.,Winkler R. 1996. Continuous wet-only and dry-only deposition measurements of 137Cs and 7Be: An indicator of their origin. Appl. Radiat. Isotopes 47, 1135–1139.

Roupsard P., Amielh M., Maro D., Coppalle A., Branger H., Connan O., Laguionie P., Hébert D., Talbaut M. 2013. Measurement in a wind tunnel of dry deposition velocities of submicron aerosol with associated turbulence onto rough and smooth urban surfaces, Journal of Aerosol Science 55:12-24 DOI:10.1016/j.jaerosci.2012.07.006

Sehmel G.A., Hodgson,W. H. 1978. A Model for predicting dry deposition of particles and gases to environmental uurfaces, DOE Report PNLSA - 6721, Pacific Northwest Laboratory, Richland,WA.

Seinfeld J., Pandis S.N. 1998. Atmospheric chemistry and Physics – John Wiley and Sons, New York.

Stull R.B. 1988. An Introduction to Boundary Layer Meteorology, R.B. Stull ISBN 978-94-009-3027-8. Kluver Academic Publisher, 1988

Sutton O.G. 1953. Micrometeorology. McGraw-Hill Book Company, New York.

Tai H.S., Lin J.J., Noll K.E. 1999. Characterization of atmospheric dry deposited particles at urban and non-urban locations. Journal of Aerosol Science 30(8), 1057-1068.

Toda M., Sugita M. 2003. Single level turbulence measurements to determine roughness parameters of complex terrain, Journal of Geophysical Research D: Atmospheres, vol. 108, no. 12, 2003.

Todd J.F., Wong G.T.F., Olsen C.R., Larsen I.L. 1989. Atmospheric depositional characteristics of beryllium-7 and lead-210 along southeastern Virginia coast. J. Geophys. Res. 94, 11106-11116.

Turekian K.K., Benninger L.K., Dion E.P. 1983. 7Be and 210Pb total deposition fluxes at New Haven, Connecticut and at Bermuda. J. Geophys. Res. 88, 5411-5415.

Venkatram A., Pleim J. 1999. The electrical analogy does not apply to modeling dry deposition of particles, Atmos. Environ., 33, 3075–3076, 1999.

Wesely M. L., Hicks B. 2000. A review of the current status of knowledge on dry deposition, Atmos. Environ., 34, 2261-2282, 2000.

WMO. 2010. Guide to Meteorological Instruments and Methods of Observation, World Meteorological Organization WMO-No. 8 2010.

Zhang L., Gong S., Padro J., Barrie L. 2001. A size-segregated particle dry deposition scheme for an atmospheric aerosol module, Atmos. Environ., 35, 549-560.

***Declaration of Interest Statement**

Declaration of interests

☒ The authors declare that they have no known competing financial interests or personal relationships that could have appeared to influence the work reported in this paper.

☐The authors declare the following financial interests/personal relationships which may be considered as potential competing interests:

Highlights (for review)

- a pathway to remove pollutants in atmosphere is the dry deposition process
- modelling of dry deposition phenomena over urban canopies is performed
- comparisons were performed between deposition velocity models and experiments covering for different surface roughness conditions
- a new parametrization of Brownian diffusion resistance seems to capture the main dry deposition processes for the examined urban canopies.

Table 1. Davenport classification of terrain roughness (Davenport et al., 2000).

Class	z_o (m)	Landscape description
Roughly open	0.10	Moderately open country with occasional obstacles (e.g. isolated low buildings or trees) at relative horizontal separations of at least 20 obstacle heights.
Rough	0.25	Scattered obstacles (buildings) at relative distances of 8 to 12 obstacle heights for low solid objects (e.g. buildings).
Very rough	0.5	Area moderately covered by low buildings at relative separations of 3 to 7 obstacle heights and no high trees.
Skimming	1.0	Densely built-up area without much building height variation.
Chaotic	2.0	City centres with mix of low and high-rise buildings.

Table 2

Table 2. Summary of experimental sites for aerosol sampling performed by ISAC-CNR. Measurement height (z), displacement height (d), and roughness length (z_0) are reported.

Site	Height z (m)	Displacement height d (m)	Roughness length z_o (m)
Venice	10	5.1 ± 0.5	0.11 ± 0.03
Bologna	10	4.8 ± 0.5	0.35 ± 0.02
Lecce	10	6.1 ± 0.4	0.53 ± 0.02
Maglie	10	6.0 ± 0.5	0.52 ± 0.02

Figure 1

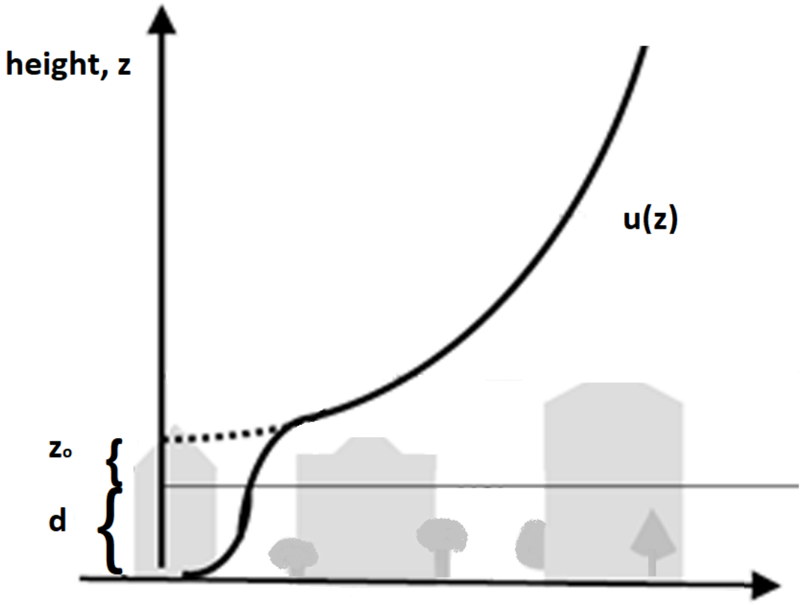

Figure 1. Profile of wind velocity, u(z), in a developed urban area. The heights are the roughness length (z_0) and the zero-plane displacement length (d).

Figure 2

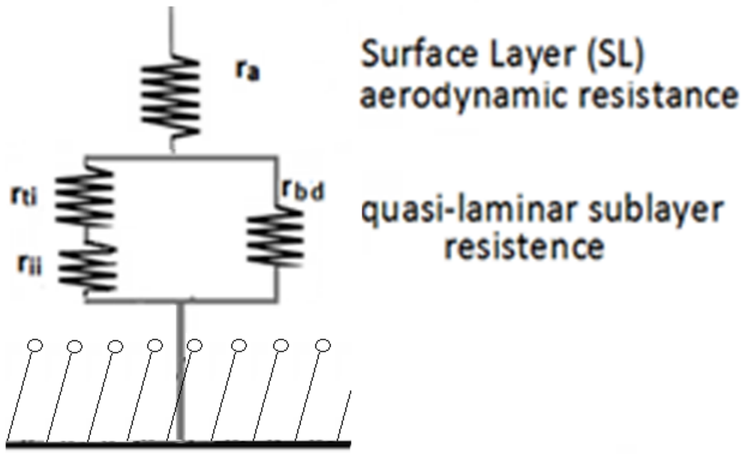

Figure 2. Electrical schematization for parametrization of particles deposition velocity reported in (Giardina et al., 2017b).

Figure 3

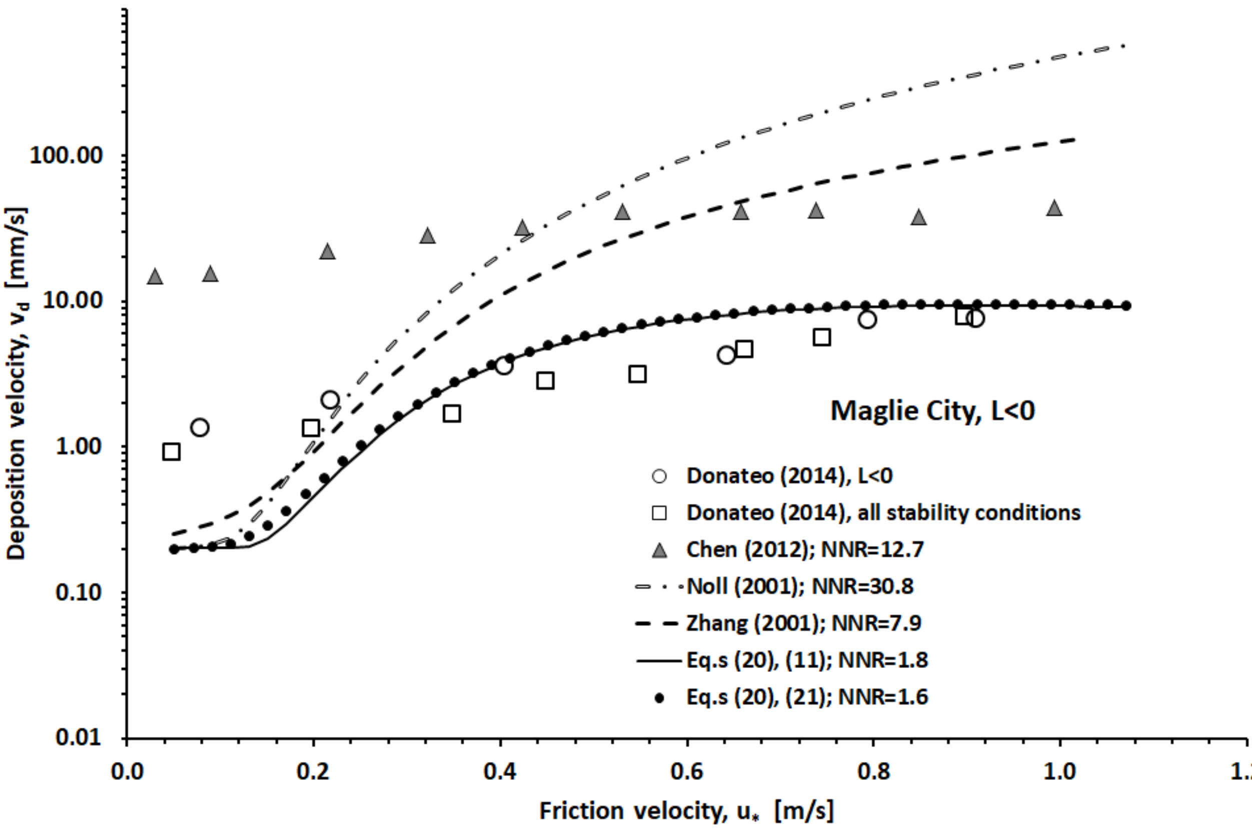

Figure 3. Comparisons among dry deposition velocity experimental data reported in (Donateo and Contini, 2014) for Maglie city, with L<0 and all stability conditions, and predictions obtained by using models reported in (Giardina et al., 2017b), (Chen et al., 2012), (Noll et al., 2001), and (Zhang et al., 2001) for d_p =2.5 μm.

Figure 4

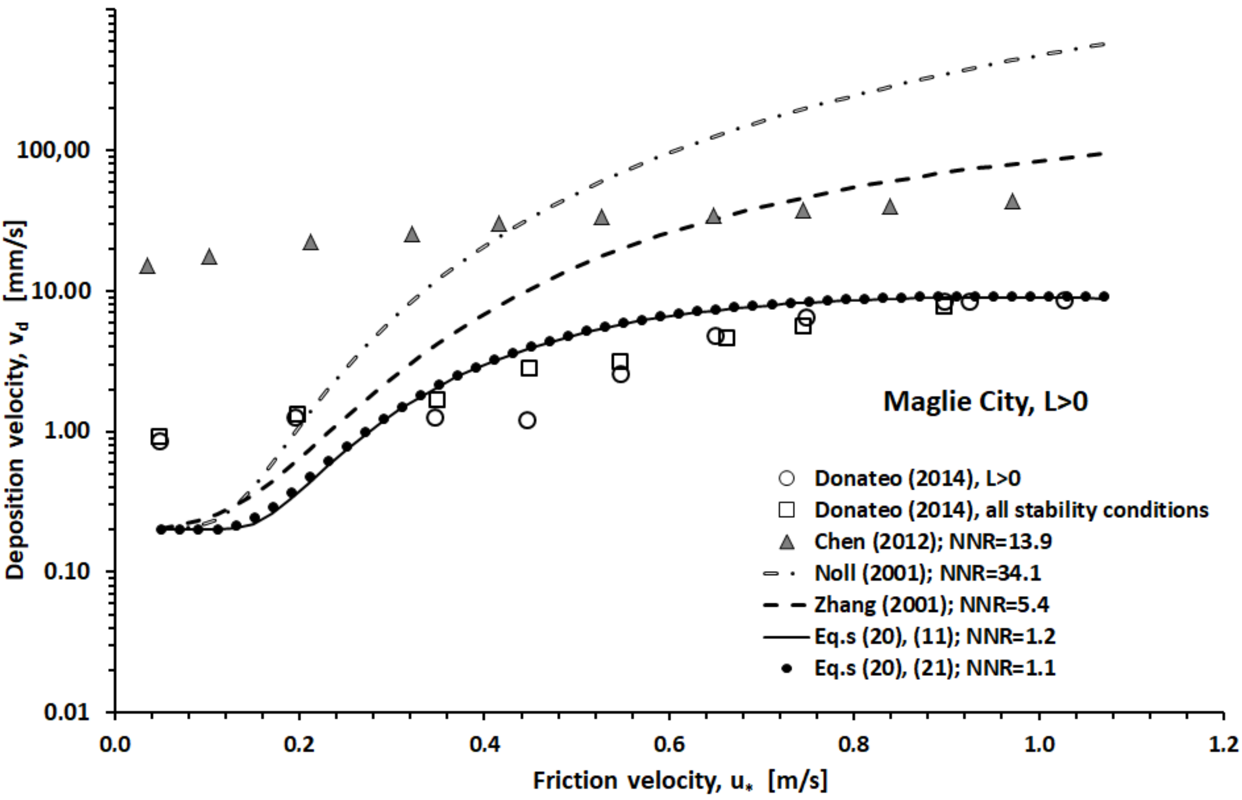

Figure 4. Comparisons among dry deposition velocity experimental data reported in (Donateo and Contini, 2014) for Maglie city, with L>0 and all stability conditions, and predictions obtained by using models reported in (Giardina et al., 2017b), (Chen et al., 2012), (Noll et al., 2001), and (Zhang et al., 2001) for d_p =2.5 μm.

Figure 5

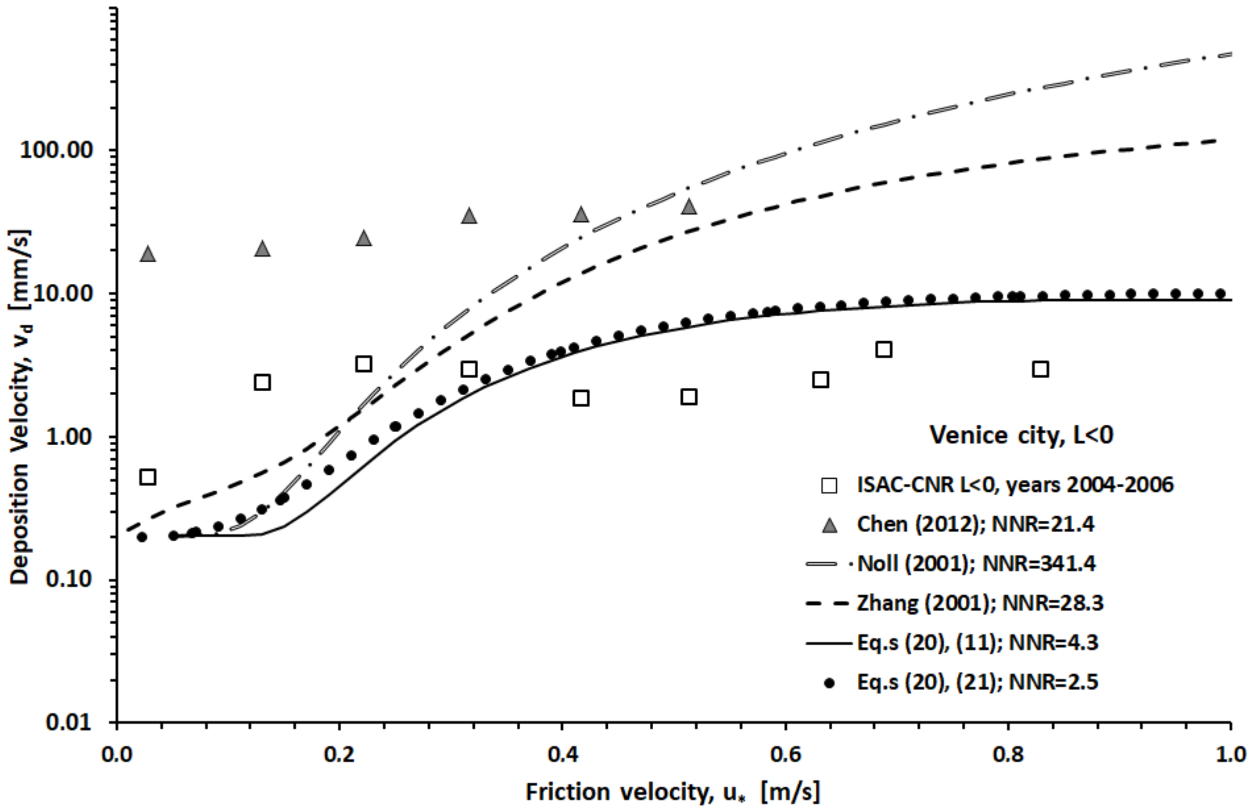

Figure 5. Comparisons between dry deposition velocity experimental data measured by ISAC-CNR for Venice, with L<0, and predictions obtained by using models reported in (Giardina et al., 2017b), (Noll et al., 2001), and (Zhang et al., 2001) for d_p =2.5 μm.

Figure 6

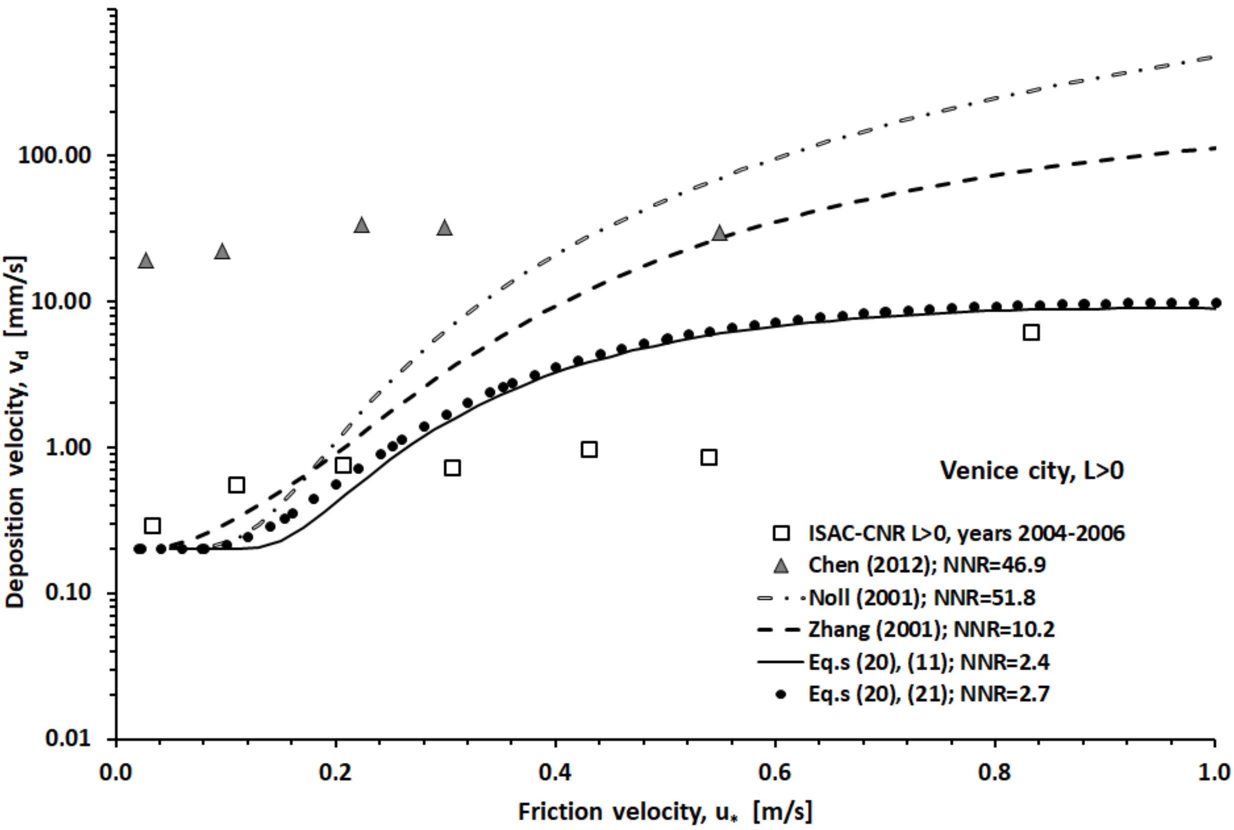

Figure 6. Comparisons between dry deposition velocity experimental data measured by ISAC-CNR for Venice, with L>0, and predictions obtained by using models reported in (Giardina et al., 2017b), (Noll et al., 2001), and (Zhang et al., 2001) for d_p =2.5 μm.

Figure 7

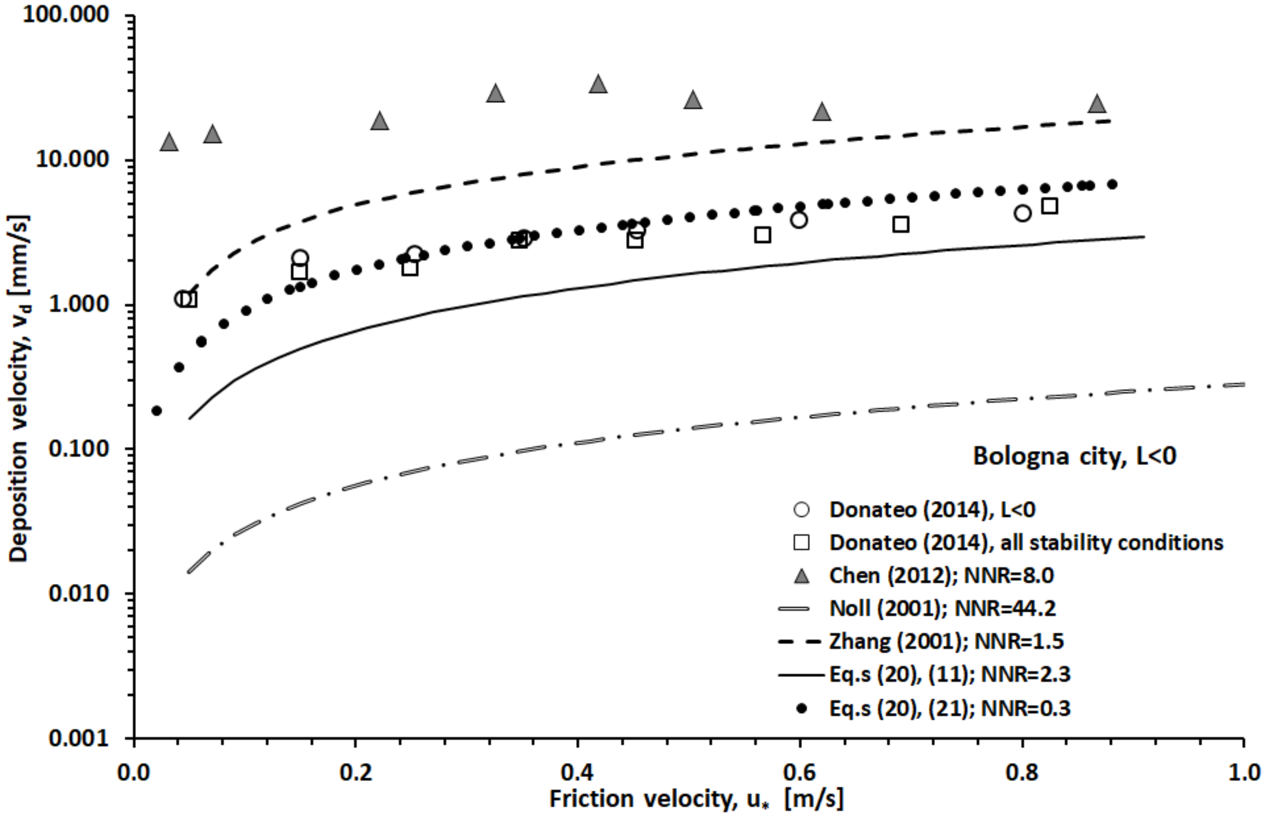

Figure 7. Comparisons among dry deposition velocity experimental data reported in (Donateo and Contini, 2014) for Bologna city outskirts, with L<0 and all stability conditions, and predictions obtained by using models reported in (Giardina et al., 2017b), (Chen et al., 2012), (Noll et al., 2001), and (Zhang et al., 2001) for d_p =0.045 μm.

Figure 8

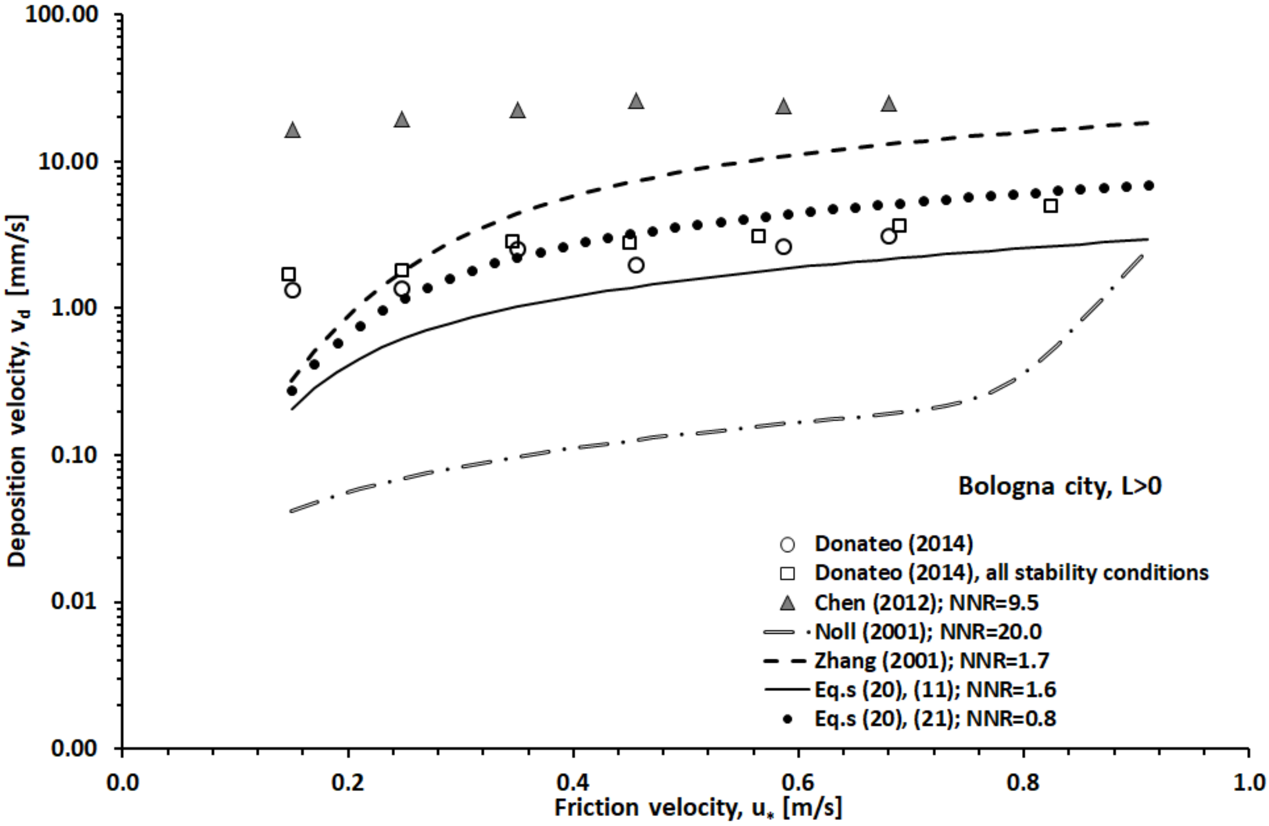

Figure 8. Comparisons among dry deposition velocity experimental data reported in (Donateo and Contini, 2014) for Bologna city outskirts, with L>0 and all stability conditions, and predictions obtained by using models reported in (Giardina et al., 2017b), (Chen et al., 2012), (Noll et al., 2001), and (Zhang et al., 2001) for d_p =0.045 μm.

Figure 9

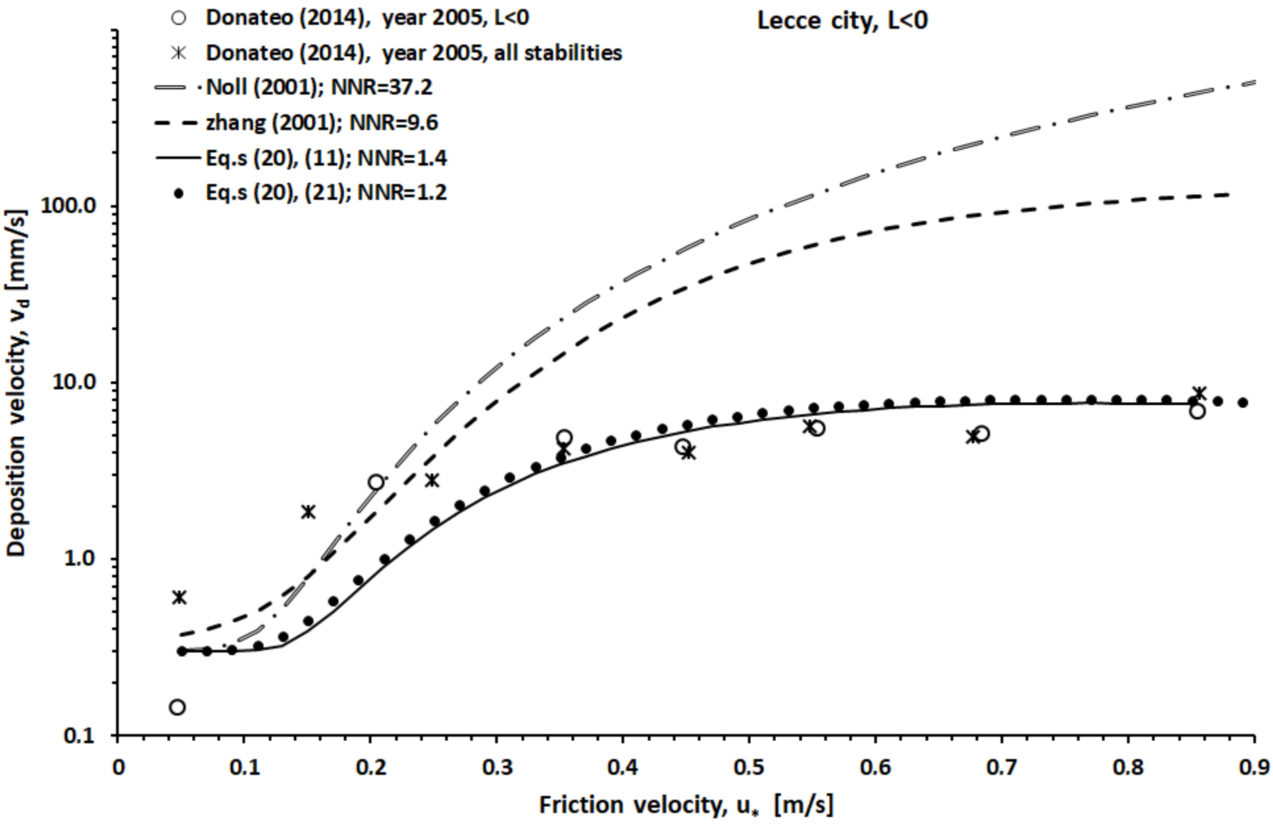

Figure 9. Comparisons among dry deposition velocity experimental data reported in (Donateo and Contini, 2014) for Lecce suburbs city, with L<0 and all stability conditions, and predictions obtained by using models reported in (Giardina et al., 2017b), (Noll et al., 2001), and (Zhang et al., 2001) for d_p =2.5 μm.

Figure 10

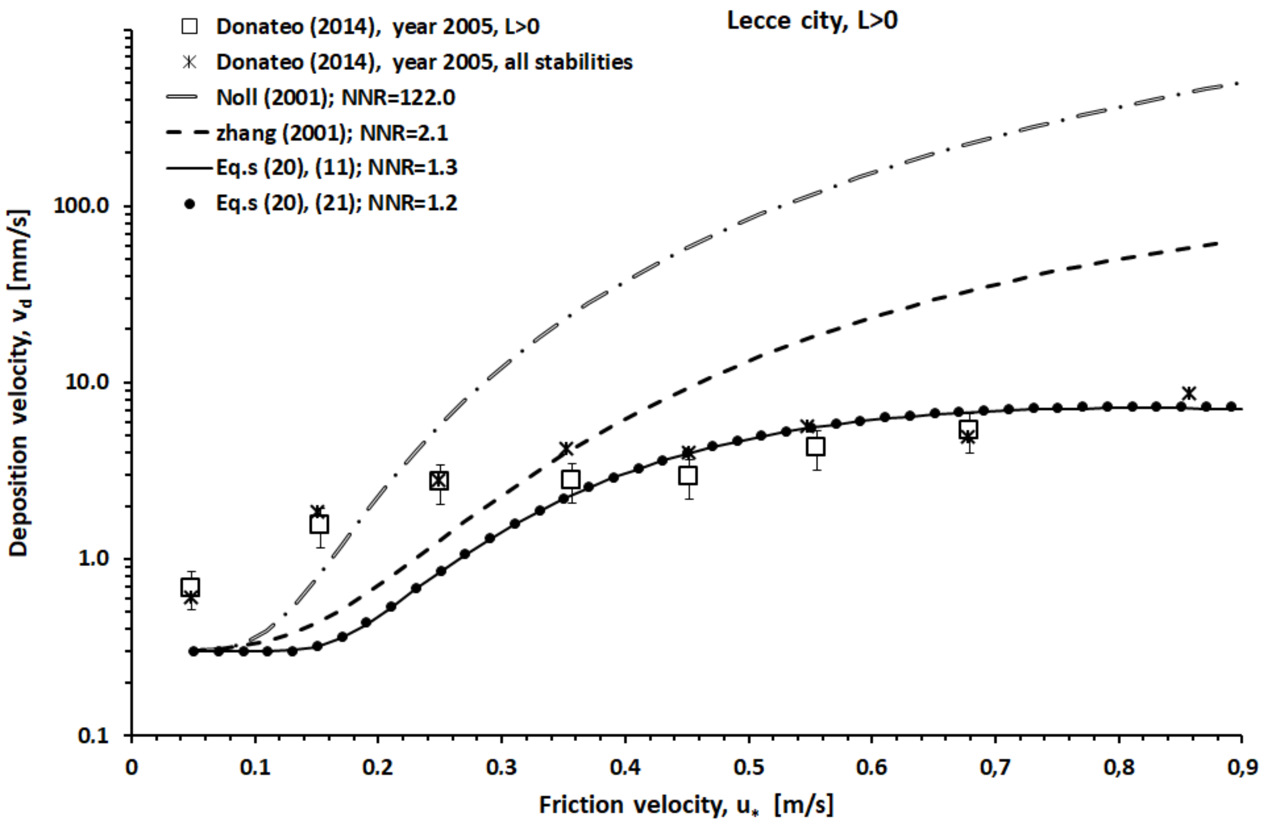

Figure 10. Comparisons among dry deposition velocity experimental data reported in (Donateo and Contini, 2014) for Lecce suburbs city, with L>0 and all stability conditions, and predictions obtained by using models reported in (Giardina et al., 2017b), (Noll et al., 2001), and (Zhang et al., 2001) for d_p =2.5 µm.

Figure 11

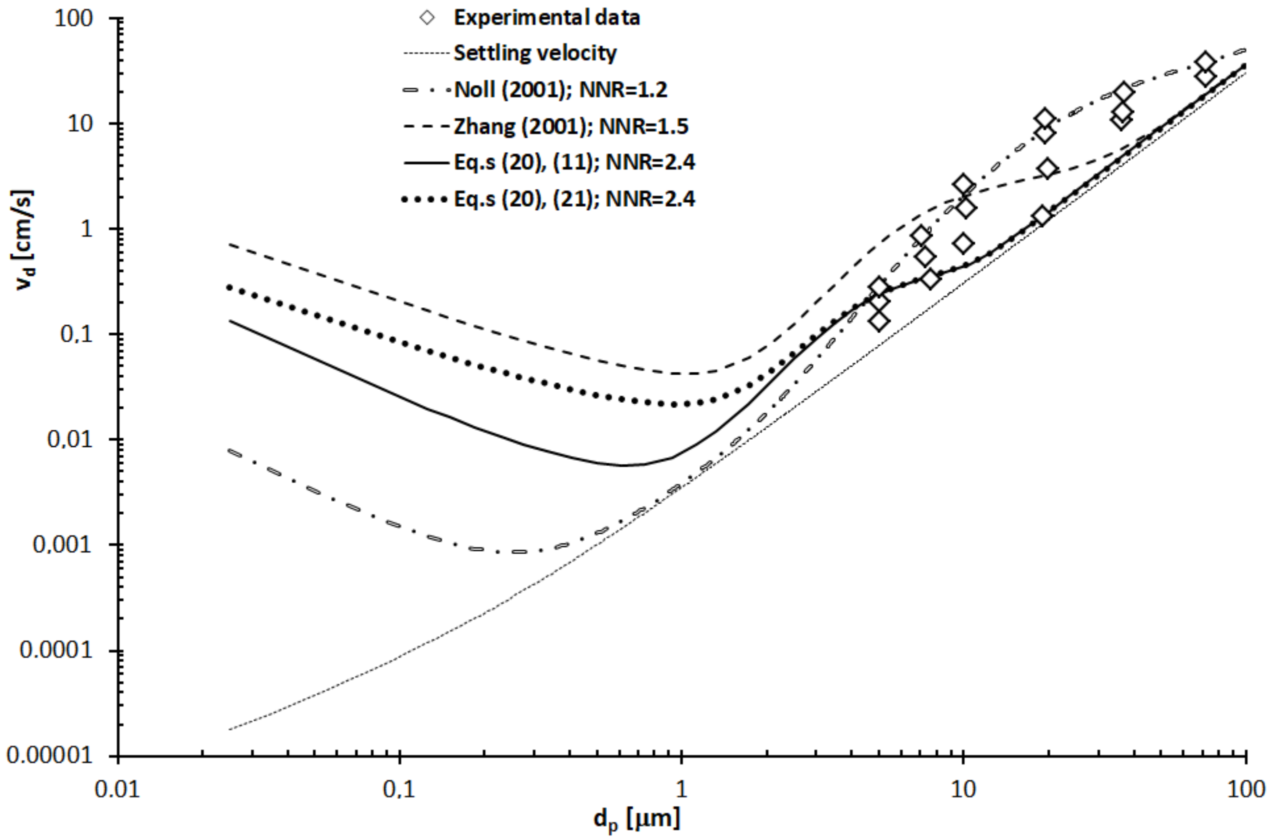

Figure 11. Comparisons between experimental dry deposition velocities reported in (Noll et al., 2001) as function of particle diameters and predictions of models reported in (Giardina et al., 2017b), (Noll et al., 2001) and (Zhang et al., 2001).

Figure 12

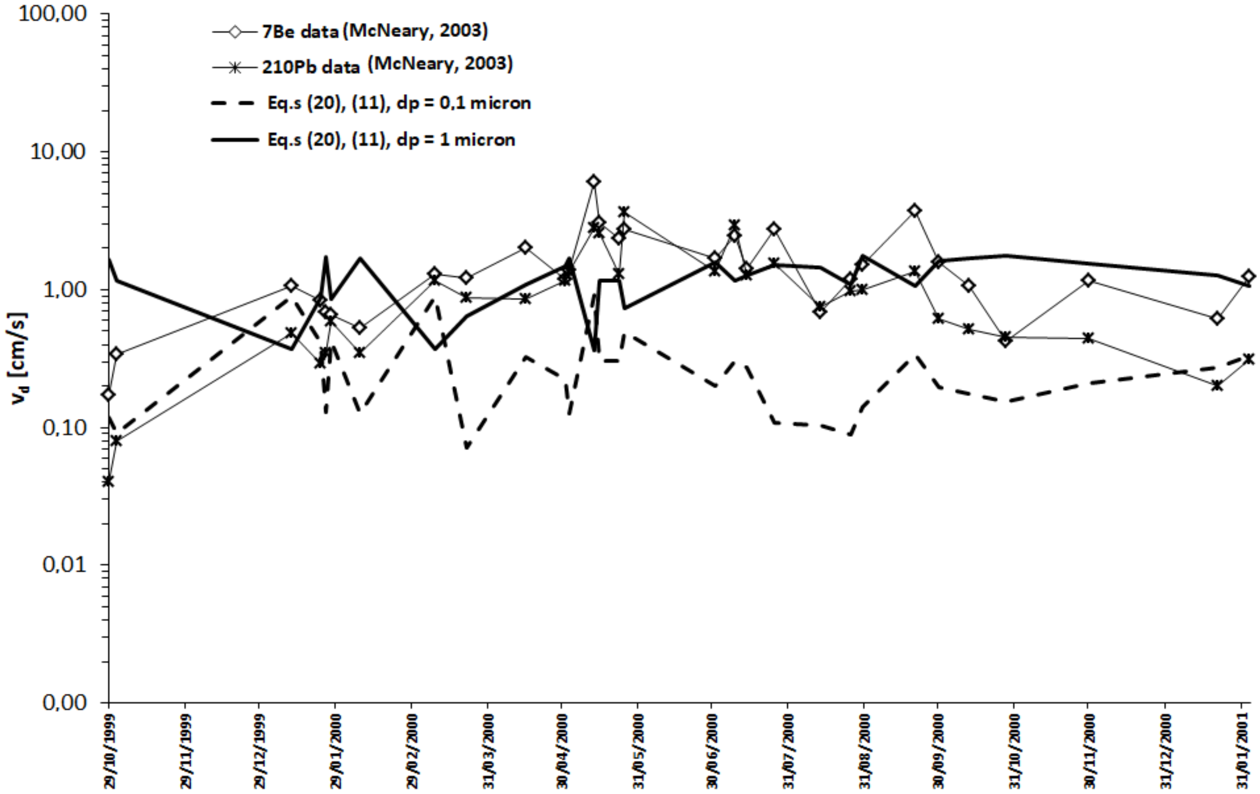

Figure 12. Comparisons between dry deposition experimental data reported in (McNeary and Baskaran, 2003) and predictions of the model proposed in (Giardina et al., 2017b) by using Brownian diffusion resistance Eq. (11) for particle diameters d_p 0.1 and 1 μm

Figure 13

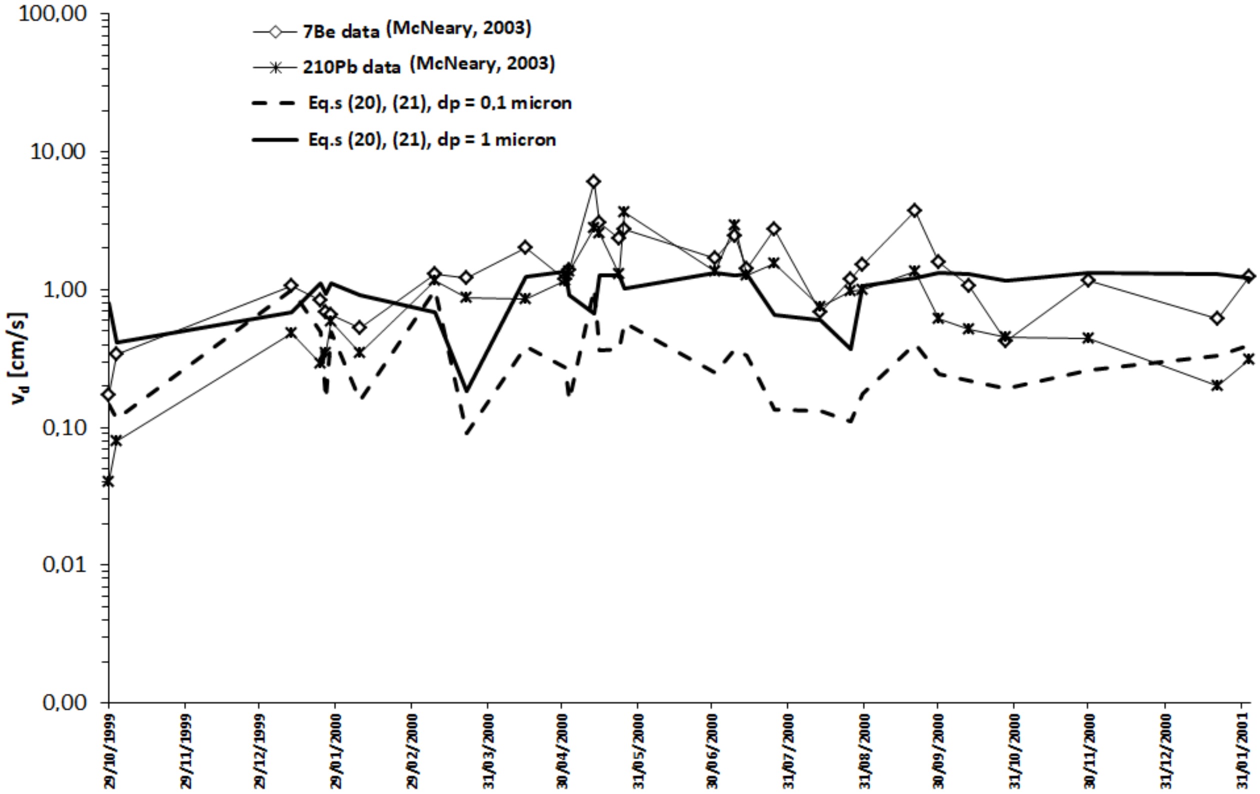

Figure 13. Comparisons between dry deposition experimental data reported in (McNeary and Baskaran, 2003) and predictions of the model proposed in (Giardina et al., 2017b) by using Brownian diffusion resistance Eq. (21) and particle diameters d_p 0.1 and 1 μm.

Figure 14

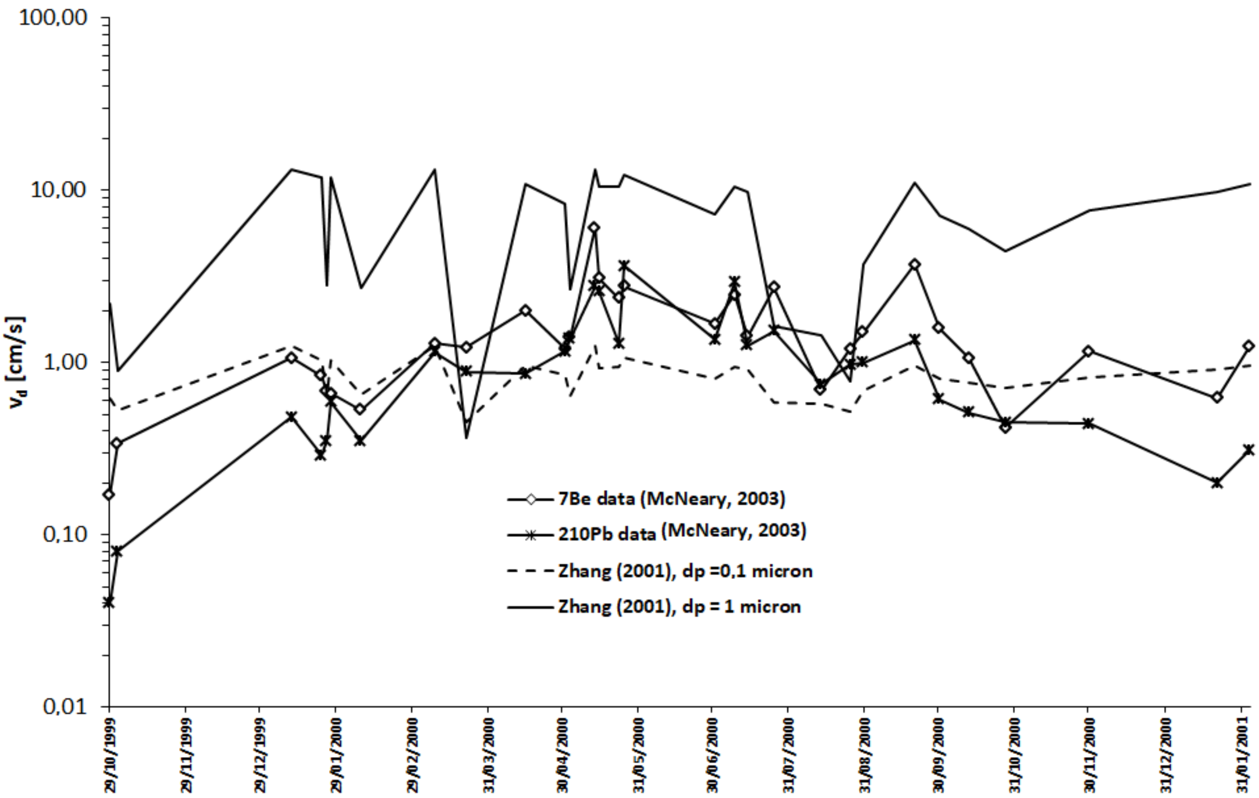

Figure 14. Comparisons between dry deposition experimental data reported in (McNeary and Baskaran, 2003) and predictions of the model proposed in (Zhang et al., 2001) for particle diameters d_p 0.1and 1 μm.

Figure 15

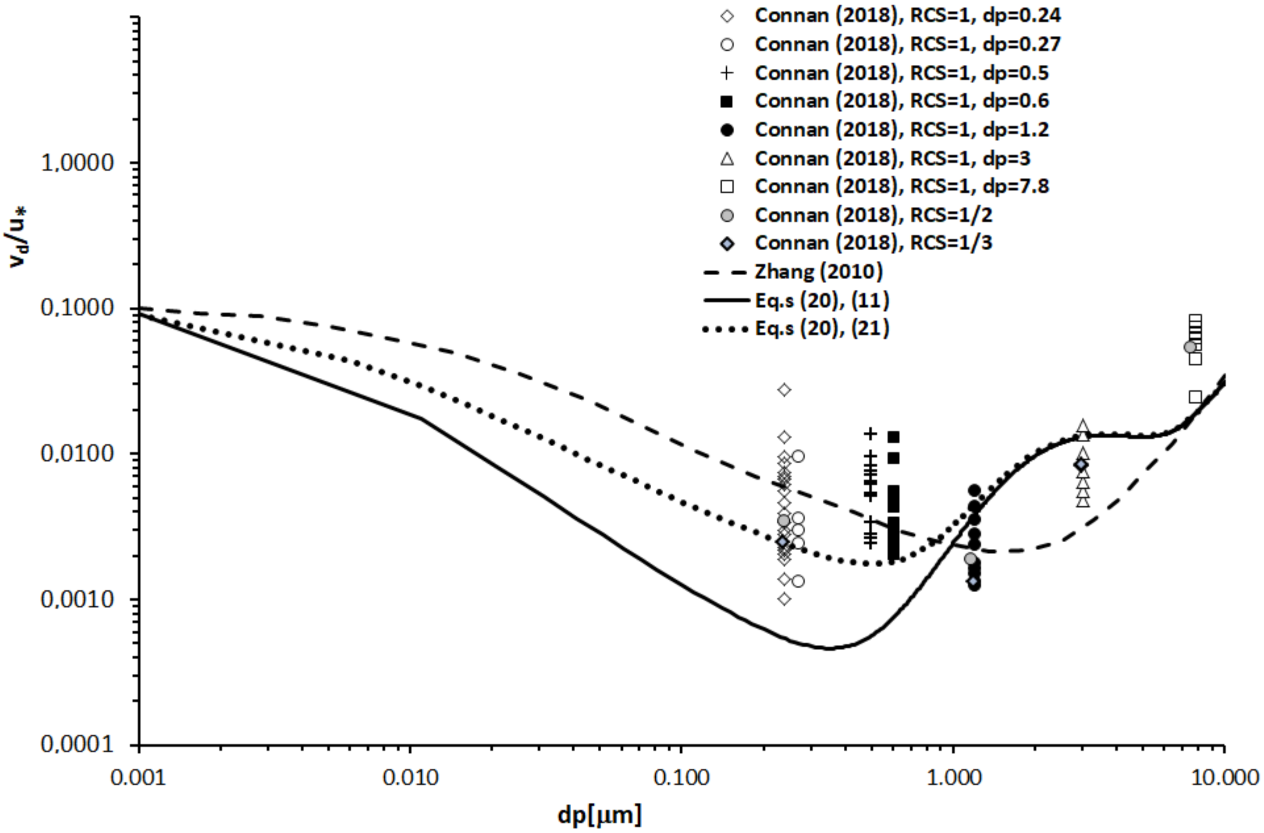

Figure 15. Comparisons between experimental data reported in (Connan et al., 2018) and predictions obtained by using (Giardina et al., 2017b) and (Zhang et al., 2001) models.